

Excess electron transport in water

R. N. Barnett, Uzi Landman, and Abraham Nitzan^{a)}

School of Physics, Georgia Institute of Technology, Atlanta, Georgia 30332

(Received 9 March 1990; accepted 16 August 1990)

The properties of excess hydrated electrons in liquid water, at room temperature, are studied via coupled quantum-classical simulations. In these simulations, the system evolves dynamically on the adiabatic potential energy surface with the electron maintained in the ground state throughout the process. The diffusion constant of the hydrated electron under field-free conditions is found to be the same as that obtained, via the Nernst-Townsend-Einstein relation, from the electron mobility simulated for a system under an electric field of 3.2×10^6 V/cm, acting on the electron. For larger electric fields, the electron mobility is found to be field dependent. The mode of migration of the excess electron is polaronic in nature and the influence of the intramolecular degrees of freedom of the water molecules on the hydrated electron transport properties is investigated. It is shown that the electron diffusion constant obtained in simulations under field-free conditions with rigid-water molecules [$D_e^0 = (3.7 \pm 0.7) \times 10^{-5}$ cm²/s] is larger than that obtained from simulations where a flexible-water model potential is employed [$D_e^0 = (1.9 \pm 0.4) \times 10^{-5}$] cm²/s] and smaller than the experimental estimated value obtained from conductivity measurements (4.9×10^{-5} cm²/s). The difference between the diffusion constants calculated for the two models is correlated with a marked enhancement of the probability of reversal of the direction of motion of the migrating electron in flexible water. The self-diffusion constant of water using the rigid-molecules model [$D_s = (3.6 \pm 0.4) \times 10^{-5}$ cm²/s] is also larger than that found for the flexible-water molecule model [$D_s = (2.3 \pm 0.2) \times 10^{-5}$] cm²/s], with the latter in agreement with the experimental value ($D_s = 2.3 \times 10^{-5}$ cm²/s). Structural and dynamical aspects of hydrated electron transport are discussed.

I. INTRODUCTION

Recent advances in theoretical methods for studies of energetics, dynamics, and spectroscopy of systems with coupled quantum and classical degrees of freedom¹ in conjunction with the development and application of experimental techniques,² such as cluster beam methods, two-photon resonant ionization, and ultrafast time-resolved spectroscopy, provide a wealth of new information about excess electrons in diverse systems. These investigations include studies of the properties and solvation dynamics of excess electrons in diverse systems such as bulk³ and clusters⁴ of polar molecules (water and ammonia), ionic salts (molten alkali halides⁵ and alkali-halide clusters^{1(e)-1(g),6}) and rare gases.^{1(b),7,8}

For polar fluid systems, studies employing quantum path-integral methods^{1(b),1(c),1(e),1(f)} and quantum molecular dynamics simulations,^{1(a),1(d),1(g)} in which the time-dependent Schrödinger equation for the electron is solved concurrently with the coupled classical equations of motion for the medium, revealed new information about the excess electron localization modes, structure, spectroscopy, and dynamics, in the bulk and in finite-size aggregates. In particular, these studies have provided overwhelming evidence for the cavity model of electron solvation⁹ in bulk polar fluids,^{1(a)} while in finite-size clusters a gradual transition

from surface to internal (cavity) localization mode has been found.^{1(d)-1(g)}

In the cavity model of solvation, the nearly spherical excess electron ground state distribution is localized in a cavity (whose radius is ~ 2 Å) surrounded by shells of the solvent molecules, with those in the inner shell (and in gradually decreasing order further shells) exhibiting preferential orientational order with respect to the center of the electron distribution in the cavity (i.e., in water the OH bonds, and in ammonia the NH bonds, of the surrounding molecules are preferentially directed towards the center of the cavity). Associated with the formation of the cavity is a significant reorganization of the polar molecular media (disruption of the hydrogen-bonded network due to cavity formation and molecular reorganization) which for bulk water at equilibrium (300 K) is estimated to be $E_R = 1.2 \pm 0.4$ eV for a flexible molecular model¹⁰ (RWK2-M) and 0.6 ± 0.3 eV for a rigid-molecular model¹¹ (RWK2), where the reorganization energy E_R is the difference between the molecular energy of the system containing the excess electron and the neutral system.

Of particular interest for investigations in solution chemistry, radiation chemistry, and the general areas of electron transport in liquids and disordered media are issues pertaining to the dynamics of excess electrons in these systems. Consequently, the migration dynamics of electrons in molten salts,^{5(a)} bulk liquid ammonia,¹² dense helium gas,¹³ and in bulk liquid water¹⁴ and water clusters¹⁵ has been recently studied. Studies of F-centerlike excess-electron migration in molten salts^{5(a)} suggest that the electron

^{a)} Permanent address: School of Chemistry, Sackler Faculty of Exact Science, Tel Aviv University, Tel Aviv 69978, Israel, and Department of Chemical Physics, Weizmann Institute of Science, Rehovot, Israel.

transport in these systems is mostly due to short-time jumps between spatially separated sites, characterized by the occurrence of configurations where at the intermediate time (between sites) the electronic wave function exhibits splitting, and it appears that a potential barrier separates the initial and final localized states of the electron. On the other hand, recent quantum molecular dynamics simulations suggest that in the case of electron diffusion in water the mode of migration is polaronic in nature.^{14,15} Thus in these systems, the electronic distribution which polarizes the local molecular solvation environment is capable of instantaneous response to changes in the local solvent configurations, resulting in spatial variations in the location of the solvated electron density (we emphasize however that in this mode of propagation, no dragging of host solvent molecules occurs¹⁵). As was discussed elsewhere,¹⁵ the difference between the electron migration mechanisms in polar molecular fluids and in molten salts may be attributed to the difference in the solvent reorganization energies and solvent dynamics. Furthermore, the enhanced diffusion of a solvated electron in water, in comparison to that of classical ions, has been shown recently¹⁴ to be related to the quantum nature of the former, which unlike the classical ions is capable of responding adiabatically to the local solvent dynamical fluctuations. In this context, it is of interest to note that studies of relaxation dynamics following excitation of an electron solvated in water yielded results¹⁶ in close correspondence to investigations of classical ion solvation dynamics, including the initial short-time (20–30 fs) reorientational stage. Thus it appears that the quantum nature of the hydrated electron is of particular significance for understanding its transport properties.

In this paper, we explore the transport properties of the hydrated electron (e_{aq}^-) in bulk water at room temperature (300 K) using coupled quantum-classical molecular dynamics simulations. These investigations extend those described in Ref. 14 in several respects: (i) study of the effects of the dynamics of the water molecules (i.e., rigid vs flexible models) on the transport properties of the electron; and (ii) studies of the mobility of the electron under the influence of an electric field acting on it. The simulation procedures and methodology are described in Sec. II.

The effect of *intramolecular* dynamics of the host water molecules on the zero-field diffusion (D_e^0) of e_{aq}^- , in thermal equilibrium, is investigated by carrying comparative simulations for rigid- and flexible-molecular models (RWK2 and RWK2-M models, respectively) of liquid water. It is found that the diffusion constant of the hydrated electron, as well as the self-diffusion of the water molecules, are larger when the rigid-water molecular model (RWK2) is employed. This behavior [which was found earlier¹⁷ for self-diffusion in water using rigid^{17(b)} and flexible^{17(a)} simple point charge (SPC) models for the water monomers] is also reflected in an enhancement of the probability for reversal of the direction of propagation of the electron in the flexible water medium. Furthermore, the mobility of e_{aq}^- under the influence of electric fields of varying strength is investigated (for the rigid-water model) and the value of the diffusion constant obtained via the Nernst–Townsend–Einstein¹⁸

(NTE) relation is compared to D_e^0 . It is found that for the smallest field employed ($f = 3.2 \times 10^6$ V/cm) the diffusion constant [$D_e = (3.4) \times 10^{-5}$ cm²/s], obtained from the electron mobility by the NTE relationship, is in agreement with D_e^0 [$(3.7 \pm 0.7) \times 10^{-5}$ cm²/s], while for higher fields a field-dependent mobility of e_{aq}^- is obtained, i.e., the electron drift velocity depends on the applied electric field in a nonlinear manner, and thus the NTE relation is not valid. These results, along with structural and dynamical aspects of the transport processes, are discussed in Sec. III. We summarize our results in Sec. IV.

II. METHOD

The simulation procedure and interaction potential which we have employed in our investigations have been described in detail in previous publications,¹⁹ therefore we limit ourself in this section to a short summary and pertinent technical details.

In our studies, we simulated a system of 256 classical water molecules at room temperature ($T = 300$ K) in a cubic calculational cell of edge length $37.28 a_0$ (i.e., at the experimental density of water 1 g/cm³) under periodic boundary conditions, interacting with an excess electron. Simulations were performed for two descriptions of water: (i) rigid water, where the equilibrium geometry of the H₂O monomer is fixed and the intermolecular interactions are given via the RWK2 model¹¹; and (ii) flexible water, where in addition to the intermolecular interactions, intramolecular interactions are given via the RWK2-M model.¹⁰ Both models have been used previously with considerable success in calculations of equilibrium properties and vibrational spectra of bulk water and water clusters,^{10,11} and in studies of electron solvation in water clusters.^{1(e)–1(g),15,16,20}

The electron–water molecule interaction was modeled by a pseudopotential which includes Coulomb, polarization, exclusion, and exchange contributions.²¹ This pseudopotential has been used by us recently in extensive studies^{1(e)–1(g),15,16,20,21} of excess electron localization modes and solvation, migration, spectra, and relaxation dynamics in water clusters of various sizes, predicting results in agreement with available experimental data.^{2(c)} All the long-range interactions (intermolecular and electron–molecule) were cut off smoothly between 9 and 9.8 Å.

The dynamics of the coupled quantum (electron)–classical (water molecules) system was simulated via the adiabatic ground-state dynamics (GSD) method.^{1(a),1(g),15,16,22} In this method, the classical time evolution of the water molecules is governed, in addition to the interatomic interactions, by the forces exerted on the molecules by the excess electronic distribution evaluated via the Hellmann–Feynman theorem. For each configuration of the solvent molecules, obtained via integration of the classical equations of motion using the velocity form of the Verlet algorithm²³ (with an integration time step 1.0365 fs for rigid water and 0.259 fs for flexible water), the ground state electronic wave function is determined by solving the time-dependent Schrödinger equation, via propagation in imaginary time. To facilitate the determination of the ground state electronic wave

function, the split-operator technique²⁴ was used with the excess electron wave function represented on a cubic grid of 16^3 points with a grid spacing of $1.5 a_0$. In order to assure that the electronic wave function is well represented (i.e., the amplitude of the wave function vanishes on the grid boundaries), we employed the moving-grid technique described previously for finite systems,^{15,16} where the wave function grid follows the diffusive motion of the electron through the calculational cell, such that the centroid of the electron density is close to the center of the wave-function grid at all times. Having obtained the electronic wave function for a given solvent configuration, it is used to evaluate the Hellmann–Feynman forces on the water molecules and subsequent integration of the classical equations of motion yields a new solvent configuration.

Simulations for both electron diffusion under zero-field conditions and electron mobility under the influence of an electric field (acting only on the electron) were performed. In the latter simulations, for an electric field strength f in the x direction, the same method outlined above was used, with the addition of the term $-efx$ to the electronic Hamiltonian.

In all our simulations, we allow the system to equilibrate at 300 K for long times (at least 3 ps) prior to collection of data (thermalization to the desired temperature is achieved via the stochastic collision method²³).

III. RESULTS

In this section, results of simulations for hydrated electron migration in bulk water are shown. We begin with a discussion of e_{aq}^- diffusion for a system at thermal equilibrium (300 K) under zero field.

A. Excess electron diffusion (zero field)

The fluctuations of the potential E_p , kinetic E_K , and total binding energy E_e of the hydrated electron, throughout the simulation, using rigid- and flexible-water models are shown in Figs. 1(a) and 1(b), respectively, and their equilibrium average values are given in Table I. As was found previously,^{14,16,21} the fluctuations in the quantum kinetic energy (E_K) reflecting the variations in the confining cavity sizes are smaller than those in the electron potential energy, which is more sensitive to fluctuations in the local solvent configurations. The fluctuations on the 20–40 fs time scale relate to the librational motion of the water molecules^{14,16} (see below). The average e_{aq}^- binding energy over the course of the simulation is $E = -2.84$ and -2.96 eV for the flexible- and rigid-water media, respectively (see Table I), in agreement with the result obtained by using a different pseudopotential for the electron–water molecule interaction and a different (rigid-molecule) description of the aqueous medium.²⁵ We also note that for the zero-field case, the values for E_p , E_K , E_e , and σ (the width of the electron distribution) are rather insensitive to the water model used (i.e., rigid or flexible molecules), while the reorganization energy E_R in the case of the flexible-water solvent is about twice as large as that of the rigid-water medium. Furthermore, analysis of the systems reveals that throughout the simulation, the separation between the energies of the ground state and the lowest

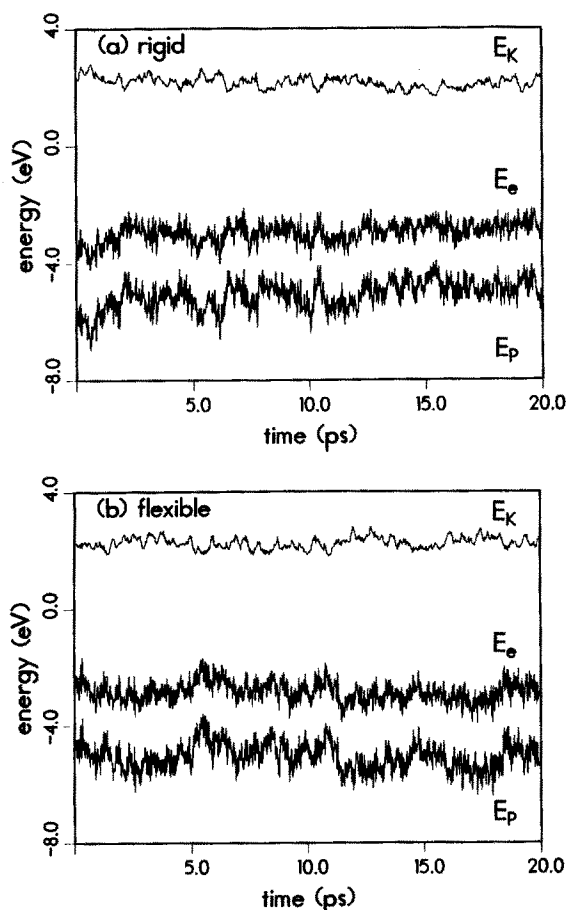


FIG. 1. The calculated potential (E_p), kinetic (E_K), and total binding (E_e) energies of an electron hydrated under zero field in bulk (a) rigid-molecule and (b) flexible-molecule water, at 300 K, vs time, for the length of the simulation. Energy is in eV and time is in ps.

excited state of e_{aq}^- is much larger than the thermal energy of the system and thus the probability for spontaneous radiationless transitions from the ground state is negligible. This provides an *a posteriori* justification for the ground-state adiabatic simulation method which we used.

Related to the above observations is the behavior of the width of the hydrated electron distribution $\sigma = R_g/\sqrt{3}$, where R_g is the radius of gyration shown in Fig. 2. As is evident, the excess electron ground-state distribution is compact ($R_g \simeq 2.2$ Å), exhibiting throughout the evolution of the systems only small fluctuations. In particular, large fluctuations, characteristic of a bimodal distribution of the electron density (such as that found for an excess electron in molten salts^{5(a)}), are absent in our system.

To investigate the field-free diffusion of the hydrated electron, we show in Figs. 3 and 4 for the rigid- and flexible-water molecules, respectively, the mean-square displacement of the centroid of the electronic distribution vs time

$$\Delta r^2(t) \equiv \langle [\mathbf{r}(t+\tau) - \mathbf{r}(\tau)]^2 \rangle, \quad (1)$$

along with the mean-square displacements of all the water molecules in the calculational cell, and those for the water molecules in the first solvation shell around e_{aq}^- . In Eq. (1), the angular brackets denote averaging over time origins and for the media averaging over water molecules as well. For a

TABLE I. Calculated properties of an electron solvated in water at 300 K and those of the solvent. Results, obtained via coupled quantum-classical simulations, for e_{aq}^- in two water solvents are given: flexible molecules (Ref. 10) and rigid (Ref. 11) molecules. For the latter one, results are given for zero field and for three values of an electric field (f) acting on the excess electron. E_p , E_K , and E_s are the potential, kinetic, and total binding energies of the solvated electron. E_R is the reorganizational energy of the solvent. D_s and D_e are the self-diffusion constant of the water molecules and the diffusion constant of the electron, respectively. D_c in the presence of finite fields is calculated from the Nernst-Townsend-Einstein (NTE) relation using the predicted electron mobility U_e [the NTE relation is not valid for the two highest fields (see the text)]. The predicted drift velocity of the electron calculated for the centroid of the electron distribution is denoted by V_d . The width of the electron distribution is given in the last column. The error estimates in square brackets were obtained via the "blocking method" (Ref. 30). The error estimates for D_e^0 (i.e., when $f=0$) were obtained by the standard deviation of the diffusion constant [slope of $r^2(t)$ vs time] calculated for the three Cartesian directions.

H ₂ O units Model	f (10 ⁶ V cm ⁻¹)	E_p (eV)	E_K (eV)	E_s (eV)	E_R (eV)	D_s (10 ⁻⁵ cm ² s ⁻¹)	D_e (10 ⁻⁵ cm ² s ⁻¹)	V_d (cm s ⁻¹)	U_e (10 ⁻³ cm ² V ⁻¹ s ⁻¹)	σ (Å)	$\sigma_{ }/\sigma_{\perp}$	t (ps)
Flexible	0	-5.07	2.23	-2.84	1.2	2.4	1.9	1.26	...	20
				[0.04]	[0.4]	[0.2]	(0.4)	[0.02]	...	
Rigid	0	-5.11	2.15	-2.96	0.6	3.5	3.7	1.28	...	20
				[0.04]	[0.3]	[0.4]	(0.7)	[0.02]	...	
Rigid	3.21	-5.09	2.18	-2.90	0.6	3.0	3.4	4.1	1.3	1.28	1.00	20
				[0.04]	[0.3]	[0.4]	[0.9]	[0.9]	[0.3]	[0.04]	1.00	
Rigid	12.8	-4.91	2.16	-2.75	1.5	3.2	5.9	30.0	2.3	1.30	1.04	10
				[0.06]	[0.5]	[0.4]	[3.0]	[3.0]	[0.3]	[0.04]	1.04	
Rigid	25.6	-4.94	2.22	-2.71	2.9	3.5	8.8	87.0	3.4	1.29	1.06	5
				[0.08]	[0.7]	[0.4]	[8.0]	[8.0]	[0.3]	[0.06]	1.06	

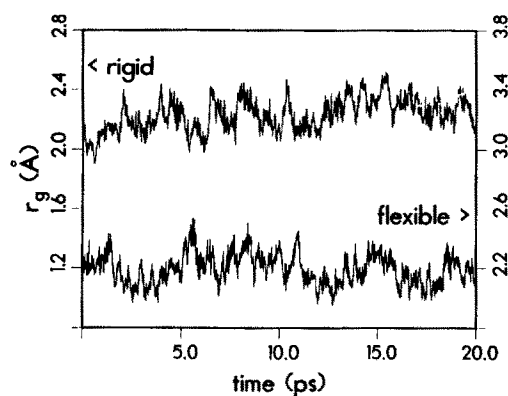


FIG. 2. Radius of gyration ($R_g = \sqrt{3}\sigma$) of the distribution of an electron hydrated under zero field in flexible (right) and rigid (left) water media, at 300 K, vs time, for the length of the simulation. R_g is in Å, time is in ps.

diffusive process $\lim_{t \rightarrow \infty} [\Delta r^2(t)/t] = 2n_d D$, where n_d denotes the number of spatial dimensions and D is the diffusion constant.²⁶

Several characteristic features should be noted from inspection of Figs. 3 and 4. In both media, the behavior of $\Delta r^2(t)$ for the molecular constituents changes at ~ 0.35 ps, with a linear relationship vs time established for larger times. Below that time, the motion is not diffusive in nature and reflects intermolecular vibrations (indeed the density of vibrational states of water²⁷ exhibits a peak at ~ 0.01 fs⁻¹). We observe that the diffusion constant of e_{aq}^- [determined from the slope of $\Delta r^2(t)$ vs t at large time, i.e., $t > 0.35$ ps], as well as the self-diffusion constant of the water molecules (solid lines), are larger in the rigid-water medium (cf. Figs. 3 and 4; see the values in Table I). Furthermore, we note that in both cases the water molecules in the first solvation shell (dashed lines) diffused faster than in the rest of the liquid (solid line).

The value of the diffusion constant under zero-field conditions D_e^0 for the electron hydrated in the rigid-molecule

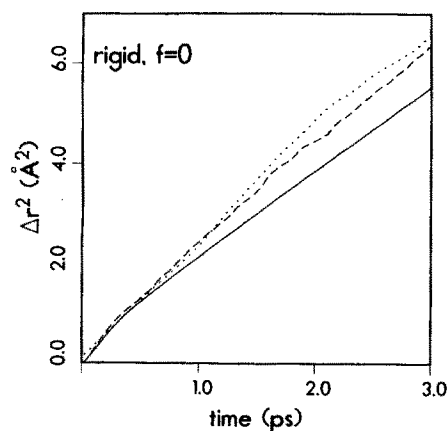


FIG. 3. Mean-square displacements [$\Delta r^2(t)$] of the hydrated electron in rigid-molecule water, at 300 K, under field-free conditions (dotted line), oxygens of the molecules in the first solvation shell of e_{aq}^- (dashed line), and that of the rest of the oxygens (solid lines) vs time. Note the change in behavior of $\Delta r^2(t)$ at ~ 0.35 ps.

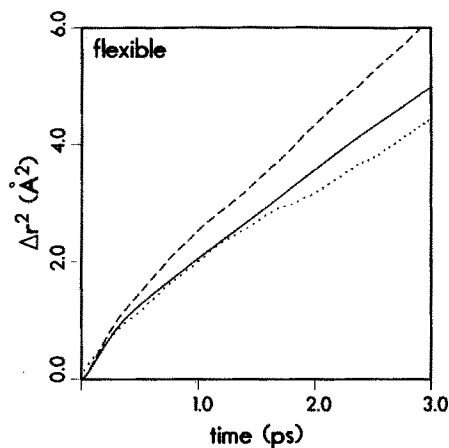


FIG. 4. The same as Fig. 3 for e_{aq}^- in a flexible-water medium.

medium (RWK2) at 300 K, $D_e^0 = 3.7 (0.7) \times 10^{-5} \text{ cm}^2/\text{s}$ [where the value in round brackets indicates the error estimate obtained as the standard deviation for diffusion in the three Cartesian directions calculated from the slopes of $\Delta r^2(t)$ for 2.5 ps time intervals] is in agreement with that obtained in a previous simulation ($D_e^0 = 3.3 \times 10^{-5} \text{ cm}^2/\text{s}$), using the rigid SPC water model²⁸ and a pseudopotential for the electron–water interaction,¹⁴ and both are smaller than the experimental estimate²⁹ obtained via the NTE relation ($4.9 \times 10^{-5} \text{ cm}^2/\text{s}$). The value obtained for e_{aq}^- in a flexible-water (RWK2-M) medium is smaller yet [$1.9(0.4) \times 10^{-5} \text{ cm}^2/\text{s}$].

The self-diffusion coefficient of the water molecules obtained from our simulations of e_{aq}^- in the rigid-molecule medium [$D_s = 3.5(0.4) \times 10^{-5} \text{ cm}^2/\text{s}$] with the error estimate obtained by the “blocking method”³⁰ is also larger than that obtained using the flexible-water model [$D_s = 2.4(0.2) \times 10^{-5} \text{ cm}^2/\text{s}$] with the latter in agreement with the experimental value at 25 °C ($D_s = 2.3 \times 10^{-5} \text{ cm}^2/\text{s}$) and with that ($D_s = 2.54 \times 10^{-5} \text{ cm}^2/\text{s}$) obtained in simulations of water using a flexible SPC model.^{17(a)} In this context, we note that in separate simulations, at 300 K, of neutral bulk water employing rigid- and flexible-water molecules, we obtained similar results $D_s = 3.6(0.4) \times 10^{-5}$ and $2.3(0.2) \times 10^{-5} \text{ cm}^2/\text{s}$, respectively. We remark that the value of D_s obtained in our simulation with the rigid-molecule model is in agreement with previous calculations employing a variety of rigid-molecule water potentials.^{14,17} Furthermore, the fact that the self-diffusion of water^{14,17} is overestimated and the diffusion of classical ions in water³¹ is underestimated in rigid-water models has been emphasized previously, and the dynamical origins of the dependence of simulated properties on the potential models employed is open for further investigations.

The difference between e_{aq}^- diffusion in rigid and flexible liquid water is seen in another way in Fig. 5, where the probability distributions for displacements of the centroid of the electron density during various time spans ($\Delta t \geq 400 \text{ fs}$) are shown. For e_{aq}^- diffusion in rigid water [Fig. 5(a)], the peak of the distribution shifts gradually and monotonically to larger distances for increasing time spans Δt . In contrast, in

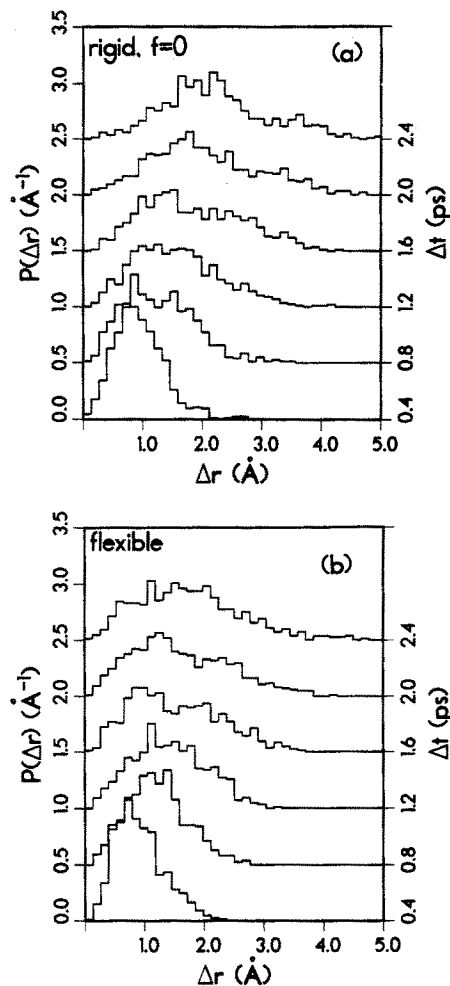


FIG. 5. Probability distributions [$P(\Delta r)$] for e_{aq}^- in (a) rigid and (b) flexible water, at 300 K, under zero field, vs displacement (Δr). In each case, $P(\Delta r)$ for different time spans Δt [0.4, 0.8, 1.2 ps, ... (see the right axis)] are shown. Note, for e_{aq}^- in flexible water (b), the motion of the peak of $P(\Delta r)$ to a lower value of Δr for $\Delta t \geq 1.6$ ps, compared to its location for $\Delta t = 1.2$ ps, indicating an enhanced probability for reversal of the direction of motion of the electron for larger times. Δr are in units of Å and $P(\Delta r)$ is in Å^{-1} (the origins of the curves for different time spans are shifted by 0.5, starting from the bottom).

the flexible medium [Fig. 5(b)], the time evolution of the distribution indicates strong back scattering, resulting in a broad distribution and in a significant probability for reversal of the direction of motion of the electron for $\Delta t \gtrsim 1 \text{ ps}$. This behavior correlates with the change in the slope of $\Delta r^2(t)$ for the electron in the flexible medium (Fig. 4) at about 1.6 ps and with the aforementioned smaller diffusion coefficient of e_{aq}^- in the flexible water host. The dynamical origin of the above phenomenon is probably associated with the significantly larger reorganization energy in the flexible water, presenting a larger resistance to the local structure change needed for the electron propagation. This larger reorganization energy is reflected also in the self-diffusion of water (with the self-diffusion constant smaller in the flexible medium as compared to that obtained in a medium described by rigid molecules) and in the relaxation dynamics as expressed, e.g., in the dielectric relaxation behavior.

The short-time ($t < 0.1$ ps) dynamics of the system [see Figs. 6(a) and 6(b) for e_{aq}^- in the flexible- and rigid-water solvents, respectively] is nondiffusive and is characterized by the librations of the water molecules.

This short-time behavior is characteristic of liquid water.^{1(g),16} The point which we would like to emphasize is the correlation between the $\Delta r^2(t)$'s of e_{aq}^- and the molecular hydrogens [particularly those of the molecules in the first solvation shell (see dashed lines marked *H* in Fig. 6)] in the short-time regime, reflecting the adiabatic response of the hydrated electron to the librations of the surrounding molecules. We note that a similar behavior has been observed in investigations of the relaxation dynamics following an electronic transition of an excess electron in water.¹⁶

The local equilibrium structure of the liquid about the localized solvated excess electron exhibits a hydration-shell structure, shown by the pair-distribution functions $g_{e-O}(r)$ and $g_{e-H}(r)$ in Figs. 7(a) and 7(b), corresponding to the distributions of molecular oxygens and hydrogens about the centroid of e_{aq}^- , respectively. Furthermore, the water mole-

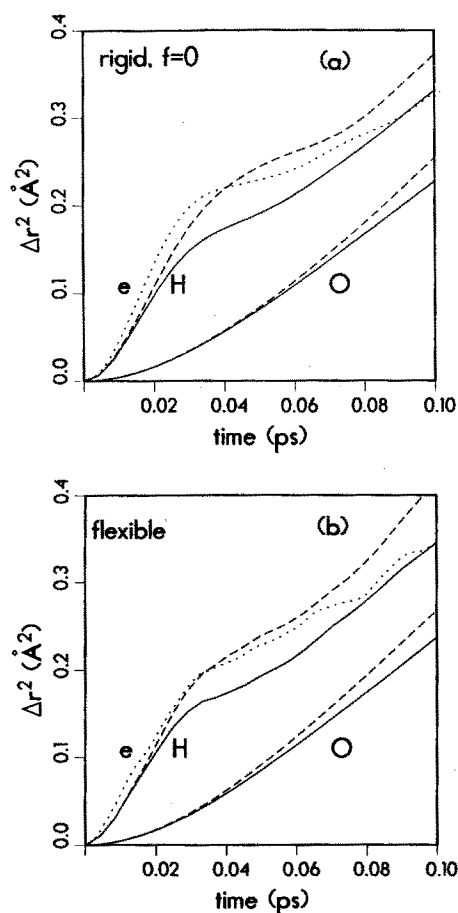


FIG. 6. Short-time dynamics of e_{aq}^- in (a) rigid and (b) flexible water, at 300 K, under zero field. $\Delta r^2(t)$ vs t are shown for the electron (dotted), hydrogens and oxygens of the molecules in the first solvation shell of e_{aq}^- (dashed lines marked *H* and *O*), and for those of the rest of the molecules (solid lines marked *H* and *O*). Note the nondiffusive character of the motion and the similarity between $\Delta r^2(t)$ of e_{aq}^- and the nearest-neighbor hydrogens indicating adiabatic following of e_{aq}^- of the librational motion of the water molecules. $\Delta r^2(t)$ is in \AA^2 and time is in ps.

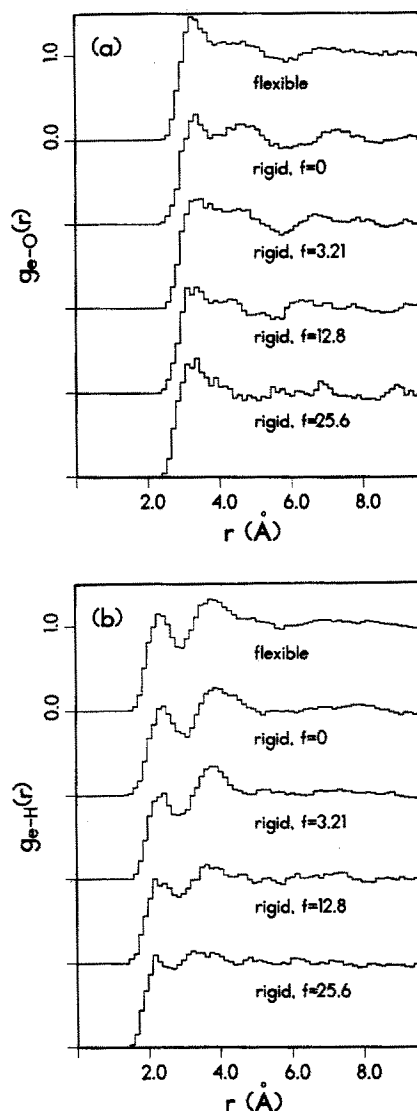


FIG. 7. Pair distribution functions $g(r)$ between the centroid of the excess electron density and the molecular oxygens (a) and hydrogens (b). Results are shown for e_{aq}^- in flexible and rigid water, at 300 K, under zero field, and for three values of an applied electric field acting on the electron hydrated in rigid water (the magnitudes of the fields f are in units of 10^6 V/cm). Note the change in the shape of the pair distribution functions as a result of the mobility of the electron under field, in particular, the broadening and obliteration of the second peak for the two highest fields [most noticeable in (b)]. All the pair distributions are normalized so that they approach unity at large distances. The distance scale is in \AA .

cules in the first solvation shell (molecules whose oxygens lie within $7.5 a_0$ from the centroid of e_{aq}^-) are preferentially oriented with one of the OH bonds directed toward the center of the e_{aq}^- solvation cavity.^{21,25}

B. Excess electron mobility

Having discussed in the previous subsection the diffusion of e_{aq}^- under zero-field conditions, we now turn to the mobility of an excess electron under the influence of an electric field. Due to the considerably larger computing effort involved in the flexible solvent case, we have limited this

study to the rigid-water medium. The electric field (f) applied in the x direction acts only on the electron (the effect of the field on the water molecule does not affect the linear response of the electron) and the dynamical ground-state evolution of the system is simulated as described in Sec. II, with the term $-efx$ added to the electronic Hamiltonian.

Simulations were performed for three electric fields $f = 3.21 \times 10^6$, 1.28×10^7 , and 2.56×10^7 V/cm. Inspection of the electronic distributions during the simulations for the above fields indicates only small distortions from the average spherical symmetry (see values of the width ratio of the electronic distribution parallel and normal to the field in Table I). Moreover, the energetics of e_{aq}^- is only slightly influenced by these electric fields (see Table I). Note, however, the influence of the two higher fields on the reorganization energy (E_R) of the solvent (see below). This strong effect is remarkable in view of the fact that the field affects the water molecules only indirectly via the motion of the solvated electron. When this motion is fast, the nearest OH groups attempt to follow the electron while the rest of the water structure cannot adjust to this local structural change. This results in a strongly nonequilibrium water structure which is reflected in the large reorganization energy.

In Fig. 8 we show the distance Δx traveled by the electron in the direction of the applied field (calculated for the centroid of the electron distribution and averaged over time origins) divided by the field strength vs time. The slopes of the curves in Fig. 8 give the electron mobilities. For small fields, the drift velocity v_d is proportional to the electric field strength, i.e., $v_d = U_e f$, with U_e the electron mobility independent of f . As seen from Fig. 8, this is not the case for the fields used in our simulations, since the different slopes correspond to field-dependent mobilities (see Table I). We note, however, that for the smallest applied electric field which we used, the value of the mobility

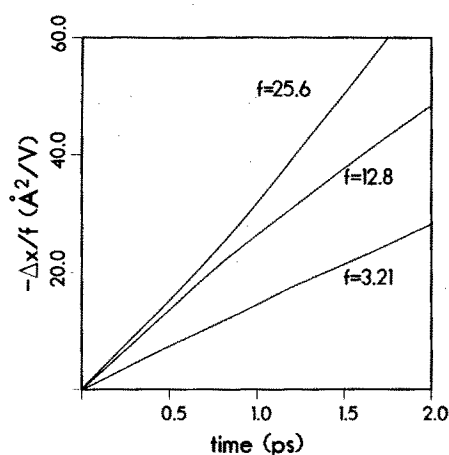


FIG. 8. The distance traveled by e_{aq}^- in the direction of the applied field, divided by the field strength ($-\Delta x/f$) vs time for an excess electron hydrated in liquid rigid water, at 300 K, vs time. The different slopes for the three fields yield field-dependent values for the corresponding mobilities. The assumptions underlying the Nernst-Townsend-Einstein relation between mobility and diffusion seem to hold only for the lowest field. ($\Delta x/f$) are in units of ($\text{\AA}^2/\text{V}$) and time is in ps. The magnitudes of the fields f are in units of $\times 10^6$ V/cm.

[$U_e = (1.3 \pm 0.3) \times 10^{-3} \text{ cm}^2 \text{ V}^{-1} \text{ s}^{-1}$] is of the same order as the experimental value²⁹ for hydrated electrons ($1.85 \times 10^{-3} \text{ cm}^2 \text{ V}^{-1} \text{ s}^{-1}$). Furthermore, using the predicted value of U_e in the NTE relation $D_e = k_B T U_e / e$ yields $D_e = (3.4 \times 10^{-5} \text{ cm}^2 \text{ s}^{-1})$, in agreement with the value obtained from our field-free simulations (see Sec. III A and Table I), indicating that for electric fields $f \lesssim 3.2 \times 10^6$ V/cm, the assumptions underlying the NTE relation¹⁸ are valid.

In this context, we note that the self-diffusion of the water molecules is only slightly affected by the field acting on the electron (see D_s in Table I).

We emphasize again that these results were obtained with the external field operating only on the electron. This procedure is valid in the linear response regime (under the same conditions where the NTE equation holds) and can also serve to indicate the onset of nonlinearity. However, our results in the nonlinear regime (the two larger applied fields) should be further examined by including the field effect on the water molecules. We defer this issue to future studies. We expect, however, that the qualitative observations described below will also hold in the modified calculation.

Next we consider the short-time dynamics of the hydrated electron acted on by the applied electric field. The calculated $\Delta r^2(t)$ for the electron and for the nearest neighbors and the rest of the hydrogens and oxygens are shown for the two lower electric fields in Figs. 9(a) and 9(b), respectively. Comparison between Fig. 9(a) and the $\Delta r^2(t)$ shown in Fig. 6(a) shows that the short-time dynamics of the system under a field of 3.21×10^6 V/cm acting on the electron, and that for field-free conditions, is very similar (i.e., nondiffusive, adiabatic response of e_{aq}^- to the librational dynamics of the solvent water molecules, in particular to the molecules in the first solvation shell). However, for the higher fields ($f = 12.8 \times 10^6$ eV/cm and even more for the highest applied field), the drifting electron is incapable of adiabatically following the librational motion, as seen from Fig. 9(b).

Related to the above behavior are differences, revealed from inspection of Fig. 7 between the local structure of the solvent around e_{aq}^- for zero-field conditions and under finite fields. Comparison between g_{e-O} and g_{e-H} for e_{aq}^- (in a rigid-water molecule solvent), for zero-field and under fields of varying strength, shows clearly that while the local solvation structure is similar for $f = 0$ and for the smallest applied field ($f = 3.21 \times 10^6$ V/cm), marked differences occur for larger fields {particularly notable in g_{e-H} [Fig. 7(b)]}. The marked change in the height and shape of the first peak of the pair distribution and the obliteration of the second peak (particularly pronounced in g_{e-H}) indicate a large perturbation of the solvation-shell structure about the excess electron drifting under the influence of the field. This perturbation, whose origin correlates with the aforementioned change in the nature of the short-time dynamics of the system for the large fields, results in a disruption of the hydrogen-bonded network of the solvent molecules about the hydrated electron which reflects itself in the larger calculated reorganization energies of the medium for these fields (see Table I). Finally, we remark that these effects are related to the above-

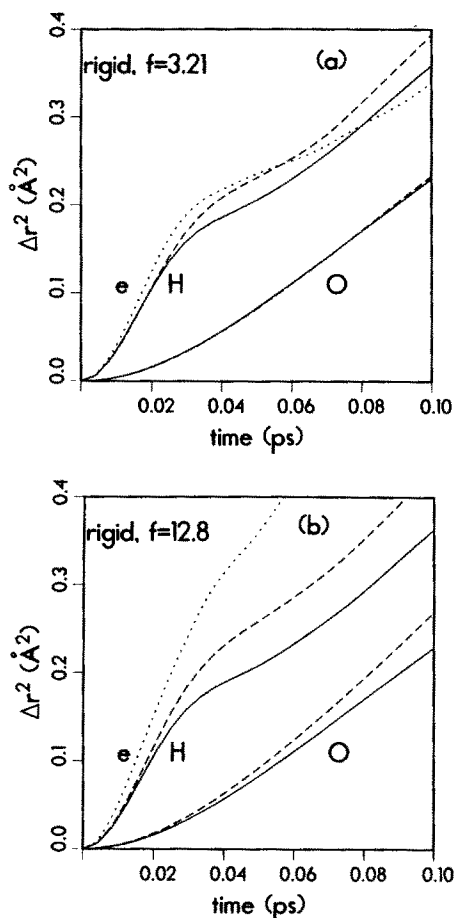


FIG. 9. Short-time dynamics of e_{aq}^- in rigid water, at 300 K, for two values of an external electric field acting on the electron: (a) 3.21×10^6 V/cm and (b) 12.8×10^6 V/cm. Designation of the different curves as given in Fig. 6. Note the similarity between (a) and Fig. 6(a) (corresponding to $f=0$), indicating that for the lowest finite field, the short-time dynamics is not influenced by the field, while for the higher field (b) the motion of e_{aq}^- does not follow the librational motion of the hydrogens.

mentioned breakdown of the assumptions underlying the NTE relation for the two highest fields.

IV. SUMMARY

The main results of our investigation of electron diffusion and mobility in liquid water, at 300 K, may be summarized as follows:

(i) Our simulations of electron diffusion in liquid water under zero-field conditions show that in a rigid-molecule model of water,¹¹ the diffusion constant of the hydrated electron as well as the self-diffusion constants of the water molecules are larger than those in a flexible-molecule medium.¹⁰ This difference is also reflected in the enhancement of the probability for reversal of the direction of motion of the electron in the flexible-molecule medium and is related to the different reorganization energies in the two model solvents and to different solvent relaxation rates in the two models.

(ii) The value of the electron diffusion constant under zero field $D_e^0 = 3.7(0.7) \times 10^{-5}$ cm²/s in the rigid-mole-

cule (RWK2 model¹¹) solvent is in agreement with previous adiabatic simulations¹⁴ which employed the rigid SPC water model and a different pseudopotential for the electron-water interaction. Both the above result and that obtained by us from adiabatic simulations using a flexible-molecule (RWK2-M model¹⁰) medium [$D_e^0 = 1.9(0.4) \times 10^{-5}$ cm²/s] are smaller than the experimental estimate (4.9×10^{-5} cm²/s) from conductivity measurements.

(iii) The self-diffusion coefficient of the water molecules using the flexible-molecule RWK2-M water model¹⁰ [$D_s = 2.4(0.2) \times 10^{-5}$ cm²/s] is in agreement with the experimental value ($D_s = 2.3 \times 10^{-5}$ cm²/s) and with calculations employing a flexible version of the SPC water model.^{17(a)}

(iv) The short-time ($t < 0.1$ ps) dynamics of the system is nondiffusive, with the electron responding adiabatically to the librational motions of the surrounding water molecules.

(v) The mode of migration of the electron is polaronic in nature,^{14,15} with the excess electron distribution polarizing the local solvent environment, and responding adiabatically to fluctuations in the local solvent configurations. Throughout the dynamical evolution of the system, fluctuations in the width of the electron distribution are small. This mode of migration differs from that suggested from simulations of electron diffusion in a molten salt.^{5(a)}

(vi) The diffusion constant calculated, using the Nernst-Townsend-Einstein relation, from the electron mobility, obtained via adiabatic simulations with a field $f = 3.21 \times 10^6$ V/cm acting on the electron, is in agreement with that calculated for electron diffusion under zero field in a rigid-molecule medium.

(vii) For higher electric fields ($f = 1.28 \times 10^7$ and 2.56×10^7 V/cm), a nonlinear relationship between the calculated drift mobilities and the applied field is found. While for the smallest field ($f = 3.21 \times 10^6$ V/cm) energetic, structural, and dynamical characteristics are very similar to those found for zero-field conditions, major differences are observed for the two higher fields. Thus, for the higher fields, the short-time ($t < 0.1$ ps) dynamics of the system does not exhibit adiabatic coupling between the electron motion and the librations of the water molecules and the solvation-shell structure about the drifting excess electron is markedly perturbed, resulting in a large increase in the reorganization energy of the medium and a decrease in the vertical electron binding energy (see E_R and E_e in Table I). These results should be reexamined in a model which includes the direct electric field action on the water molecules.

ACKNOWLEDGMENTS

This research was supported by U.S. Department of Energy Grant No. FG05-86ER45234, by the Israel Academy of Science, and by the U.S.-Israel Binational Science Foundation.

¹ See reviews in: (a) P. J. Rossky and J. Schnitker, *J. Phys. Chem.* **92**, 4277 (1988); (b) B. J. Berne and D. Thirumalai, *Annu. Rev. Phys. Chem.* **37**, 401 (1986); (c) M. Sprik and M. Klein, *Comp. Phys. Reports* **7**, 147

- (1988); (d) R. Kosloff, *J. Phys. Chem.* **92**, 2087 (1988); (e) R. N. Barnett, U. Landman, D. Scharf, and J. Jortner, *Acc. Chem. Res.* **22**, 350 (1989); (f) J. Jortner, D. Scharf, and U. Landman, in *Elemental and Molecular Clusters*, edited by G. Benedek, T. P. Martin, and G. Pacchioni (Springer, Berlin, 1989), p. 148; (g) R. N. Barnett, U. Landman, G. Rajagopal, and A. Nitzan, *Isr. J. Chem.* **30**, 85 (1990).
- ² See reviews in: (a) M. M. Kappes and S. Leutwyler, in *Atomic and Molecular Beam Methods*, edited by G. Scoles (Oxford University, London, 1989); (b) R. L. Whetten and M. Y. Hahn, in *Atomic and Molecular Clusters*, edited by E. R. Bernstein (Elsevier, Amsterdam, 1989); (c) J. V. Coe, G. H. Lee, J. G. Eaton, S. T. Arnold, H. W. Sarkas, K. H. Bowen, C. Ludewigt, H. Haberland, and D. R. Worsnap, *J. Chem. Phys.* (in press); (d) A. Migus, Y. Gauduel, J. L. Martin, and A. Antonetti, *Phys. Rev. Lett.* **58**, 1559 (1987).
- ³ See Refs. 1(a)–1(c), 2(d), and references therein.
- ⁴ See Refs. 1(b), 1(e)–1(g), 2(a)–2(c), and references therein.
- ⁵ (a) A. Selloni, P. Carenvali, R. Car, and M. Parrinello, *Phys. Rev. Lett.* **59**, 823 (1987); (b) M. Parrinello and A. Rahman, *J. Chem. Phys.* **80**, 860 (1985).
- ⁶ G. Rajagopal, R. N. Barnett, A. Nitzan, U. Landman, E. C. Honea, P. Labastie, M. L. Homer, and R. L. Whetten, *Phys. Rev. Lett.* **64**, 2933 (1990).
- ⁷ G. J. Martyna and B. J. Berne, *J. Chem. Phys.* **88**, 4516 (1988).
- ⁸ H. Haberland, T. Kolar, and T. Reiners, *Phys. Rev. Lett.* **63**, 1219 (1989).
- ⁹ See reviews by: (a) N. R. Kestner, in *Electron–Solvent and Anion–Solvent Interaction*, edited by L. Kevan and B. C. Webster (Elsevier, Amsterdam, 1976), p. 1; (b) *Electrons in Fluids*, edited by J. Jortner and N. R. Kestner (Springer, New York, 1973), p. 1, and references therein.
- ¹⁰ J. R. Reimers and R. O. Watts, *Chem. Phys.* **85**, 83 (1984).
- ¹¹ J. R. Reimers, R. O. Watts, and M. L. Klein, *Chem. Phys.* **64**, 95 (1982).
- ¹² M. Sprik and M. L. Klein, *J. Chem. Phys.* **89**, 1592 (1988); M. Sprik and M. L. Klein, *J. Chem. Phys.* **91**, 5665 (1989).
- ¹³ R. K. Kalia, P. Vashishta, and S. W. de Leeuw, *J. Chem. Phys.* **90**, 6802 (1989).
- ¹⁴ J. Schnitker and P. J. Rossky, *J. Phys. Chem.* **93**, 6965 (1989).
- ¹⁵ R. N. Barnett, U. Landman, and A. Nitzan, *Phys. Rev. Lett.* **62**, 106 (1989); *J. Chem. Phys.* **91**, 5567 (1989).
- ¹⁶ R. N. Barnett, U. Landman, and A. Nitzan, *J. Chem. Phys.* **90**, 4413 (1989).
- ¹⁷ (a) J. Anderson, J. J. Ullo, and S. Yip, *J. Chem. Phys.* **87**, 1726 (1987); (b) For a comparative study of liquid water employing several rigid-molecule models, see W. L. Jorgensen, J. Chandrasekhar, J. D. Madura, R. W. Impey, and M. L. Klein, *ibid.* **79**, 926 (1983).
- ¹⁸ See discussion in E. A. Mason and E. W. McDaniel, *Transport Properties of Ions in Gases* (Wiley, New York, 1988).
- ¹⁹ See Ref. 1(g), 15, and 16, and references therein.
- ²⁰ R. N. Barnett, U. Landman, S. Dhar, N. R. Kestner, J. Jortner, and A. Nitzan, *J. Chem. Phys.* **91**, 7797 (1989).
- ²¹ R. N. Barnett, U. Landman, C. L. Cleveland, and J. Jortner, *J. Chem. Phys.* **88**, 4421 (1988); **88**, 4429 (1988).
- ²² R. N. Barnett, U. Landman, and A. Nitzan, *J. Chem. Phys.* **84**, 2242 (1988).
- ²³ J. R. Fox and H. C. Anderson, *J. Phys. Chem.* **88**, 4019 (1984).
- ²⁴ M. D. Feit, J. A. Fleck Jr., and A. Steiger, *J. Comput. Phys.* **47**, 412 (1982).
- ²⁵ J. Schnitker and P. J. Rossky, *J. Chem. Phys.* **86**, 3462 (1987); **86**, 3471 (1987).
- ²⁶ This formula is due to A. Einstein, in *Investigations on the Theory of the Brownian Movement*, edited by R. Furth (Methuen, London, 1926). This book contains five of Einstein's important papers on the subject.
- ²⁷ R. N. Barnett, U. Landman, and A. Nitzan, *J. Chem. Phys.* **93**, 6535 (1990).
- ²⁸ H. J. C. Berendsen, J. P. M. Postma, W. F. Gunsteren, and J. Hermans, in *Intermolecular Forces*, edited by B. Pullman (Reidel, Dordrecht, 1981).
- ²⁹ (a) K. H. Schmidt and W. L. Buck, *Science* **151**, 70 (1966); (b) G. C. Barker, P. Fowles, D. C. Sammon, and B. Stringer, *Trans. Faraday Soc.* **66**, 1498 (1970); (c) See review by W. F. Schmidt in Ref. 9(a); (d) E. J. Hart and M. Anbar, *The Hydrated Electron* (Wiley, New York, 1970).
- ³⁰ H. Flyvberg and H. G. Petersen, *J. Chem. Phys.* **91**, 461 (1989).
- ³¹ (a) G. I. Szosz, W. O. Riede, and K. Z. Heinzinger, *Z. Naturforsch. Teil A* **34**, 1083 (1979); (b) G. Palinkas, W. O. Riede, and K. Z. Heinzinger, *ibid.* **32**, 1137 (1977); (c) M. Migliore, S. L. Fornili, E. Spohr, and K. Z. Heinzinger, *ibid.* **42**, 227 (1982); (d) M. Berkowitz and W. Wan, *J. Chem. Phys.* **85**, 376 (1987); (e) M. R. Reddy and M. Berkowitz, *ibid.* **88**, 7104 (1988); M. A. Wilson, A. Pohorille, and L. R. Pratt, *ibid.* **83**, 5832 (1985).